Technical Note TN-36

THE MAGNETIC SUSCEPTIBILITY OF SOILS IS DEFINITELY COMPLEX

J. Duncan McNeill

April, 2013

The Magnetic Susceptibility of Soils is Definitely Complex.

1. Introduction

It has been noticed in many archaeological surveys with the Geonics EM 38B that the measured susceptibility (in-phase) anomalies also showed a coincident, paired (but normally of different amplitude) negative anomaly in the conductivity (quadrature phase) data. The similarity in shape of these paired anomalies showed that a common phenomenon was causing both responses and that the coincident quadrature phase anomalies were not caused by changes in terrain conductivity.

It was clear that the soil susceptibility response was often 'complex' in that the quadrature phase response was due to a time lag in the overall susceptibility response caused by what is known as soil 'magnetic viscosity'.

This Technical Note is based mainly on the work of Néel (1949) and Mullins and Tite (1973). Néel showed that the magnetic susceptibility of an assemblage of thinly dispersed magnetic grains in a non-magnetic matrix, such as soil, often lags application of a static magnetic field. The reason is that crystal structure of ferrimagnetic minerals such as magnetite and maghemite renders the crystal anisotropic, with both easy and difficult directions of magnetization. Two different easy directions will be separated by an energy barrier that must be surmounted before the direction of magnetization can be changed from one easy direction to another, causing a delay in the response.   The height of this energy barrier is a function of the volume of the mineral grains, with the result that larger grains take longer than smaller grains to align themselves with the inducing field. Since there will be a wide assortment of grain volumes in a soil, there will be a wide variation in the grain response times. However if the magnetic minerals are disperse enough, the overall response is simply the sum of the responses from individual magnetic grains.

 Both Néel and Mullins and Tite assumed in their calculations and measurements that the sum is to be taken over an infinite continuous distribution of different response times. Others have assumed that there is a finite distribution of response times. In this Technical Note we have performed calculations to see how well these models agree with measured data.

We also propose an interpretative technique for complex susceptibility measurements which may allow calculation of magnetite mineral grain size from the quadrature phase component of EM 38B survey data.

For background material, the results of many new archaeological surveys with the EM 38B are described in two recent Geonics Technical Notes, TN 34 and TN 35, available by accessing the Geonics website at www.geonics.com, and proceeding to Library and Technical Notes.

2. Basic Theory--Magnetic Viscosity

In this Technical Note we assume, as did Néel, that naturally occurring, very small, single-domain (SD) size grains of magnetic minerals (such as magnetite and maghemite) exhibit what is known as 'magnetic viscosity'. Single-domain refers to the fact that the entire magnetization in a single mineral grain points in the same direction (a magnetic domain). Magnetically changing this direction requires rotation of the entire domain to the new direction, requiring energy expenditure to overcome internal forces in the crystal structure which slows the reorientation process. Magnetic viscosity is apparent when it is observed that the induced (secondary) magnetic field in a rock or soil sample is unable to follow the time-variation of the inducing (primary) magnetic field in either the time-domain or frequency-domain.

Néel shows that τ , the observed time-lag, or relaxation 'time-constant' in the response from a single-domain mineral grain, is a strongly varying function of the domain volume V , given by

$$\tau = A\exp(VJ_sH_c/2kT) \tag{1}$$

where A = constant

V = grain (domain) volume

J_s = spontaneous magnetic moment of the grain

H_c =coercive magnetic force of the grain
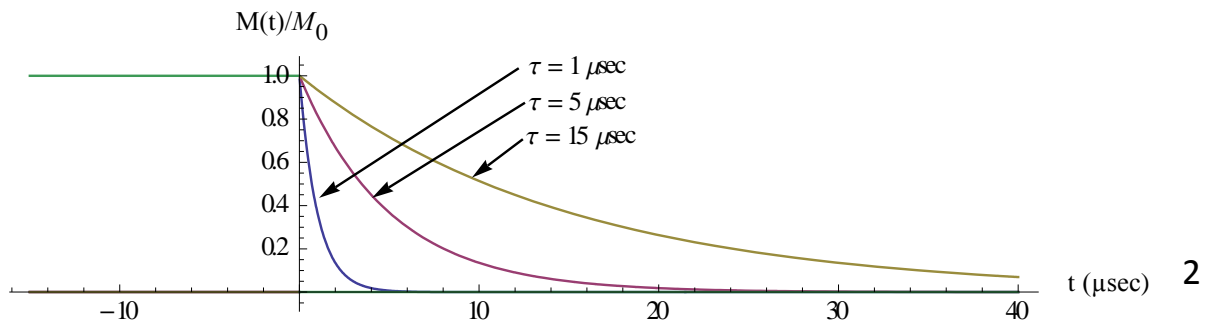
k =Boltzmann constant

T =absolute temperature

and $(VJ_sH_c/2)$ is the energy required to overcome the energy barrier.

Note from equation (1) that if $J_sH_c/kT \gg 1$, very small differences in grain volumes in a sample will produce an enormous range of grain time-constants.

If an assemblage of SD grains all having the same time-constant τ has been magnetized by a constant uniform primary magnetic field of strength M_0 which is abruptly terminated at time t =0, Néel states that the remanent magnetization of the assemblage effectively decays with time t as

$$M(t)/M_0 = \exp(-t/\tau) . \tag{2}$$

The following figure shows this transient behavior (i.e. the delayed response) for three SD assemblages with different time-constants of 1, 5, and 15 μ sec .
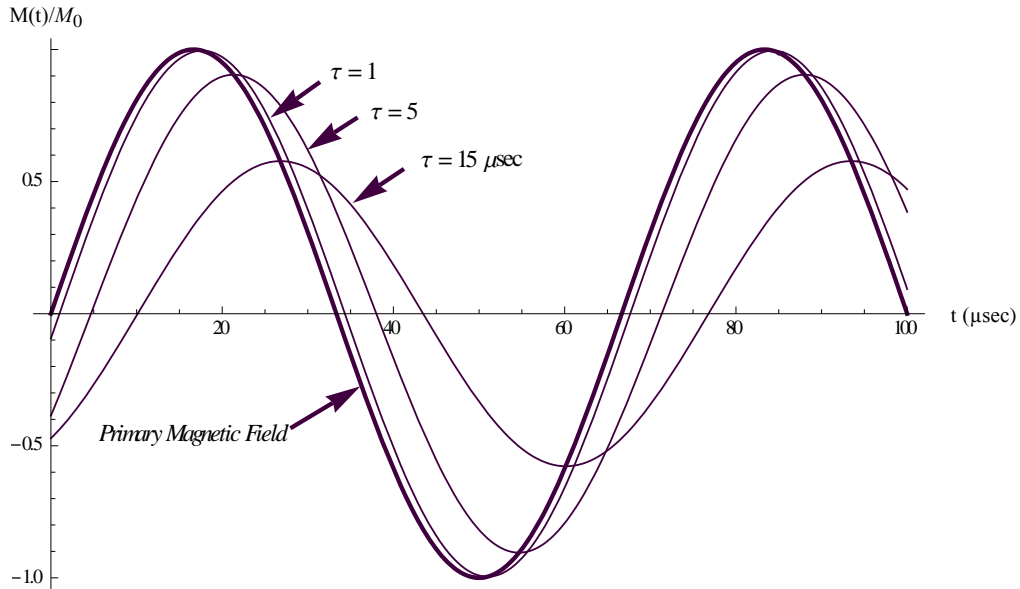
However the Geonics EM 38B operates in the frequency-domain rather than the time-domain, so we are also interested in how the time response given in equation (2) appears when the primary magnetic field varies sinusoidally with time, i.e. as $M_0 \sin(\omega t)$, where $\omega = 2\pi f$, and f is the frequency of the primary magnetic field (15 kHz for the EM 38B). Taking the Fourier transform of the impulse response corresponding to the step-function response equation (2) yields the result that

$$M(\omega)/M_0 = \frac{1}{\tau}\frac{1}{((1/\tau)+j\omega)}e^{j\omega t} = \frac{(1-j\omega\tau)}{(1+(\omega\tau)^2)}e^{j\omega t} \tag{3}$$

where $j = \sqrt{-1}$. When expressed in trigonometric form, equation (3) becomes,

$$. \qquad M(\omega)/M_0 = \frac{\sin(\omega t)-(\omega\tau)\cos(\omega t)}{1+(\omega\tau)^2} \tag{4}$$

We are interested in the behavior of this response as a function of the excitation frequency f but we will follow normal practice of presenting equations as functions of the angular frequency $\omega = 2\pi f$. The next figure shows the behavior of the right-hand side of equation (4) for three SD assemblages with the same values of time-constant shown in the figure above.

This figure shows both the sinusoidally varying primary magnetic field and the response from the three different secondary magnetic fields. It is seen that, for the case of $\tau = 1\mu\sec$, which is much less than the time-period of one cycle of the primary magnetic field (given by the reciprocal of the operating frequency of $f = 15\ kHz$, i.e. 67 $\mu\sec$) the response is almost completely in-phase with the primary field, but that for the longer time-constants the response significantly lags the primary magnetic field. Indeed, for $\tau = 15\mu\sec$ (which is about one-quarter of the period of the primary field), the response lags

3

the primary field by about $10\mu\sec$ and essentially varies as $\cos(\omega t)$. We say that, for this long time-constant, the response is essentially in 'quadrature phase' with the sinusoidal primary magnetic field, whereas for the much shorter case of $\tau = 1$ μsec the response is said to be essentially 'in-phase' with the primary field.

We will use these phrases many times in the material that follows. The reason for this is that, as suggested by the figure and equation (4), a sinusoidal response that time-lags another reference sinusoid can always, as indicated by equation (4) be decomposed into an in-phase and quadrature phase response (or component) with respect to the reference sinusoid. Indeed this is the way that the signal detectors in the EM 38B operate. There are two such detectors; one gives the in-phase response and the other the quadrature phase response.
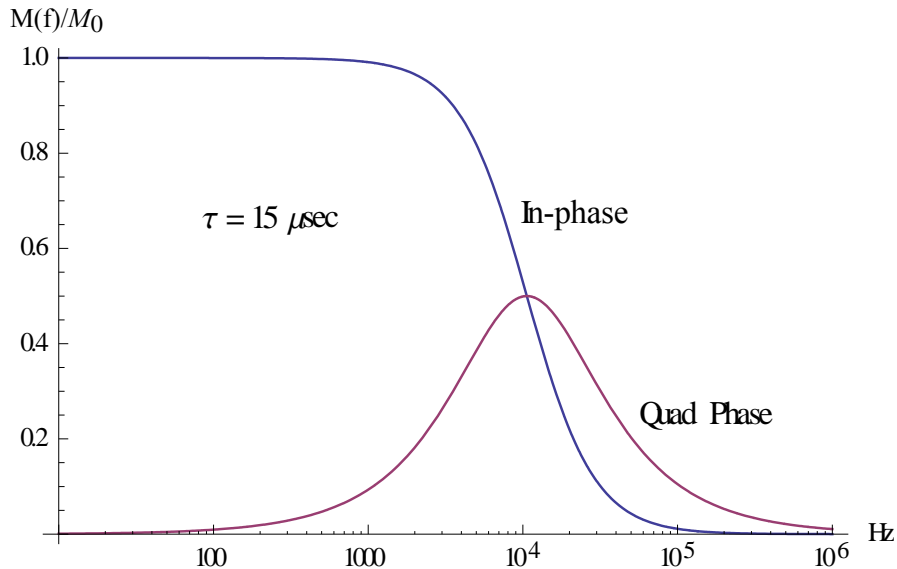
We also note from the figure that, as is indicated by equation (4), the amplitude of the response from the assemblage decreases with increasing time-constant.

The above figure described the behavior of the assemblage response as a function of time. We now examine the behavior as a function of frequency f. From equation (4) we infer that the amplitudes of the in-phase and quadrature components of the response are given by

$$In(\omega\tau) = In(2\pi f\tau) = \frac{1}{1+(\omega\tau)^2} = \frac{1}{1+(2\pi f\tau)^2} \tag{5}$$

$$Qd(\omega\tau) = Qd(2\pi f\tau) = -\frac{(\omega\tau)}{1+(\omega\tau)^2} = -\frac{(2\pi f\tau)}{1+(2\pi f\tau)^2}. \tag{6}$$
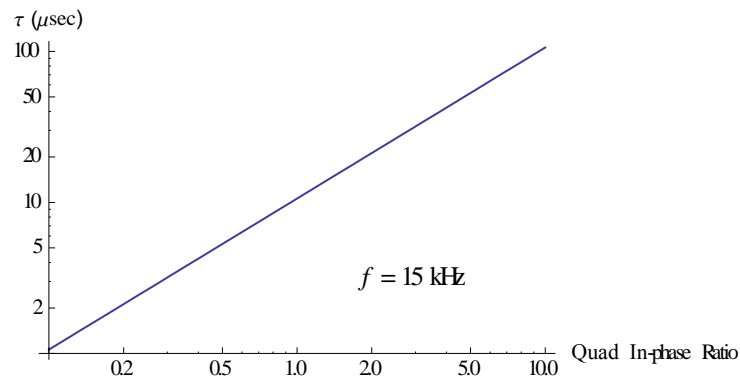
For convenience in plotting, we ignore the fact that the quadrature component is negative. We observe that the functional dependence on f always occurs in the product $(2\pi f\tau)$ so that any change in response that occurs, for example, as τ increased, will be the same as if f decreased by the same relative amount. These components are shown in the figure below for $\tau = 15\mu\sec$.

4

As would be expected, at low frequencies where the primary field period is much longer than the time-constant and thus where the response easily follows the drive frequency, the response is entirely in-phase. As the frequency increases the quadrature phase response increases, becoming a maximum at a frequency where the period is of the same order as the time-constant (actually at frequency $f = 1/(2\pi\tau)$); at still higher frequencies both components decrease to zero.

The next figure (for $f = 15\ kHz$, the operating frequency of the EM38B) shows a log-log plot of time-constant τ plotted against the ratio of quadrature phase to in-phase response, which, as shown by equation (7), is a straight line of slope proportional to this ratio.

$$\frac{Qd(f)}{In(f)} = 2\pi f \tau, \qquad \therefore \tau = \frac{1}{2\pi f}\frac{Qd(f)}{In(f)}. \tag{7}$$
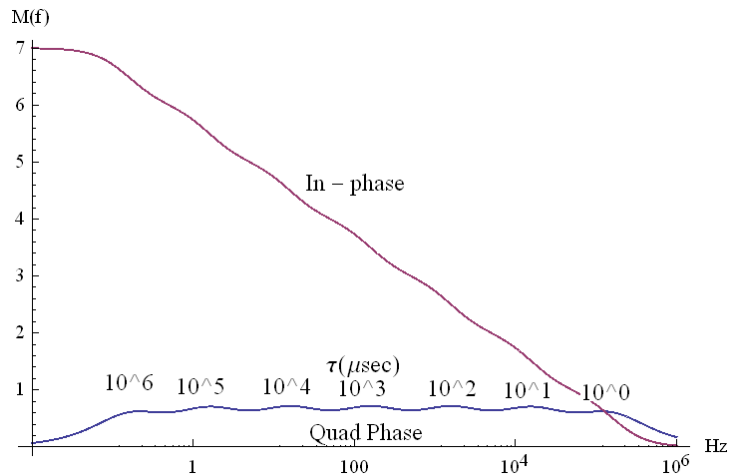

We see that if the response is exponential it is not necessary to measure the whole response curve to determine the value of the time-constant; we need only measure the quadrature phase to in-phase ratio at any frequency and perform the calculation.

We have seen, however, from equation (1) that the grain time-constant is a very sensitive function of grain volume, and in an assemblage of grains of various sizes it is clear that there will be a large number of grains of different time-constants. If these mineral grains are physically far removed from each other in the crystal structure (the ferrimagnetic component is usually a small fraction of the total, of the order of a few percent by volume) the responses from grains with different time-constants will be independent from each other; to calculate the total response of the assemblage we are justified in simply adding the responses from the individual grains. For simplicity we will also assume (as did Néel and Mullins and Tite) that apart from having different time-constants, the amplitude of the response from all grains is the same (reported measurement data shows that this restriction is not as serious as it seems; this point will be discussed later).

5

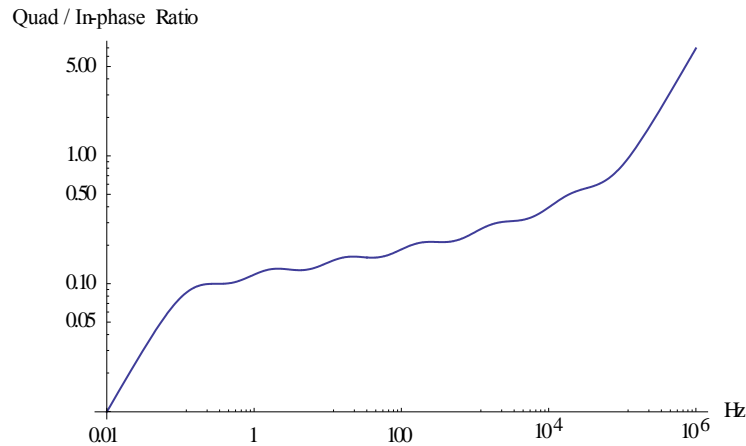## 3. 'Finite Discrete Time-Constant' Susceptibility Model

The next figure shows the frequency response of our 'finite discrete time-constant' susceptibility model. It consists of the sum of the responses from an assemblage of seven different grain sizes, the smallest with time-constant 1 $\mu\sec$, each larger size with time-constant greater by a factor of ten, and the largest with time-constant $\tau = 1\sec$.

The significant difference in this response compared with the response from a single grain is surprising. The first point to note is the relative flatness of the quadrature phase response. Moreover the factor of ten spacing between the time-constants was chosen so that in this figure the quadrature phase response would still show the separate influence from each of the seven time-constants. Had we chosen the interval ratio between each time-constant to be $\sqrt{10}$ rather than 10, the quadrature phase response would have been very smooth.

Similarly smooth is the in-phase component, which is now virtually a straight line on the log-linear plot, indicating that the in-phase response can be described by A-B $\log(f)$ where A and B are constants. The in-phase response is constant at very low frequencies where the effect of the largest time-constant has not been felt and decays slowly with higher frequencies.

The figure below shows behaviour of the quadrature/in-phase ratio for the assemblage as a function of frequency. We saw above that, for a single time-constant, the ratio of quadrature to in-phase response sufficed to define the time-constant but, as shown in the figure below, if measurements of this ratio are made in the central frequency region (where several time-constants are influencing the response at each frequency) this ratio is a slowly varying function of frequency (or of the assemblage time-constants) and measurement of this ratio produces little useful information.

Recall from Section 1 that the model used by Néel and Mullins and Tite (as well as others) employed an infinite number of time-constants. Such a model produces essentially the same response as in the two figures above, except that in their calculations the central response continues unaltered throughout the complete frequency range (there are no wings).   Our model, in which the assemblage consists of a finite number of time-constants, shows that at the low and high frequencies the frequency response is determined only by the time-constants of the longest and shortest time-constant grains. Thus the quadrature/in-phase ratio, relatively flat at intermediate frequencies, quickly becomes a linear function of frequency at both low and high frequency extremes, as it would for a single time-constant.

Indeed, we originally conjectured that the reason the EM 38B surveys were produced so many anomalies with significant quadrature phase response was that the operating frequency of this instrument was high enough, and the time-constant of the shortest time-constant grains low enough, that the response was caused only by these short time-constant grains. This figure shows, however, that if that such were the case most of the measured quadrature/in-phase ratios would be of the order of unity or greater, whereas in fact they are consistently smaller than unity.

Why does it take so few time-constants to produce the relatively smooth curves in the above two plots, particularly for the quadrature phase plot? The answer is shown by equation (6). Assuming a value for τ of $1m\sec$ equation (6) tells that the maximum value of the quadrature phase response will be 0.50 at a frequency $f = 1/(2\pi\tau) = 160\ Hz$. Furthermore, solving equation (6) to learn at which frequencies the response is one-half the maximum value (i.e. 0.25) we see that this value occurs at frequencies of both $f_L = 43\ Hz$ and $f_H = 596\ Hz$. Thus the response from a single time-constant extends over a very wide frequency range compared with the value of the central frequency. It does not take many single time-constant responses to fill in a given frequency interval. The Néel theory does not require thousands of time-constants!

Moreover , as was done on page 4, we usually plot this type of response on a log-linear plot, which is misleading since it makes the response look symmetrical about the central frequency. But this

7

calculation shows the response to be distinctly asymmetrical, extending further on the high frequency side of the central frequency. Such behaviour is evident on the plot of the quadrature phase/in-phase ratio on page 7 where it is seen that at the low frequency part of the spectrum the transition from the initial, low-frequency time-constant to the many time-constant region takes place over a smaller frequency interval than the corresponding transition from the many time-constant region to the final, high-frequency time-constant at the high-frequency end of the spectrum.

Finally we note that at the low frequency end of the spectrum this model reproduces the well-known 'percent frequency-effect' described by Clark (1989) in which the measured magnetic field from some magnetic anomalies decreases with increasing measurement frequency. Note also that at these low frequencies the amplitude of the quadrature component of the susceptibility will usually be negligible compared with the in-phase component and whether the total or the in-phase component of the susceptibility is measured will have no effect on the computed value of the 'percent frequency-effect'.

4. 'Infinite Continuous Distribution of Time-Constants' Susceptibility Model (Néel Theory)

In this Technical Note, although it is both historically inconsistent and unfair to Néel, we have commenced our extended discussion of magnetic viscosity using the 'finite discrete time-constant' susceptibility model since it permits an easy introduction to the properties of 'complex' magnetic susceptibility.   We now note that in an epochal paper Néel (1949) showed that in a ferrimagnetic sample consisting of a continuous distribution of an infinite number of time-constants of uniform amplitudes, variation of the in-phase component of magnetic susceptibility $\chi_i(\omega)$ with frequency was related to the step-function response by

$$\frac{\partial \chi_i(\omega)}{\partial \ln(\omega)} = \frac{1}{h_0} \frac{\partial \sigma_r(t)}{\partial \ln(t)} \tag{8}$$

where (using Néel's notation) σ_r is the remanent magnetization previously acquired in a magnetic field of strength h_0, and $\chi_i(\omega) = M_i(\omega) / M_0$. Néel also showed theoretically that the induced remanent magnetization of an infinite assemblage decays with time as $\ln(t)$.

In another important paper Mullins and Tite (1973) further developed Néel's theory of magnetic viscosity to include the behaviour of quadrature phase susceptibility, and also reported initial measurements to confirm the extended version of the theory. They showed that the quadrature phase component of the magnetic susceptibility was related to the right-hand side of equation (8) by

$$\chi_q = \frac{-\pi}{2h_0} \frac{\partial \sigma_r(t)}{\partial \ln(t)} \tag{9}$$

and thus that

$$\chi_q = -\frac{\pi}{2} \frac{\partial \chi_i(\omega)}{\partial \ln(\omega)} . \tag{10}$$

These features are shown in Section 3 to also be true for an extended *finite* assemblage.

Mullins and Tite present a short table of measured results of the frequency behavior of both the in-phase and quadrature phase components of the magnetic susceptibility over a frequency range 66 to 900 Hz; their results are in good agreement with equation (10) for single-domain grains, confirming the general accuracy of the Néel theory (as has since been demonstrated by other workers over the years). However we note that the Néel theory is inconsistent with survey experience with the EM 38B which, as described later often produces anomalous quadrature/in-phase responses.

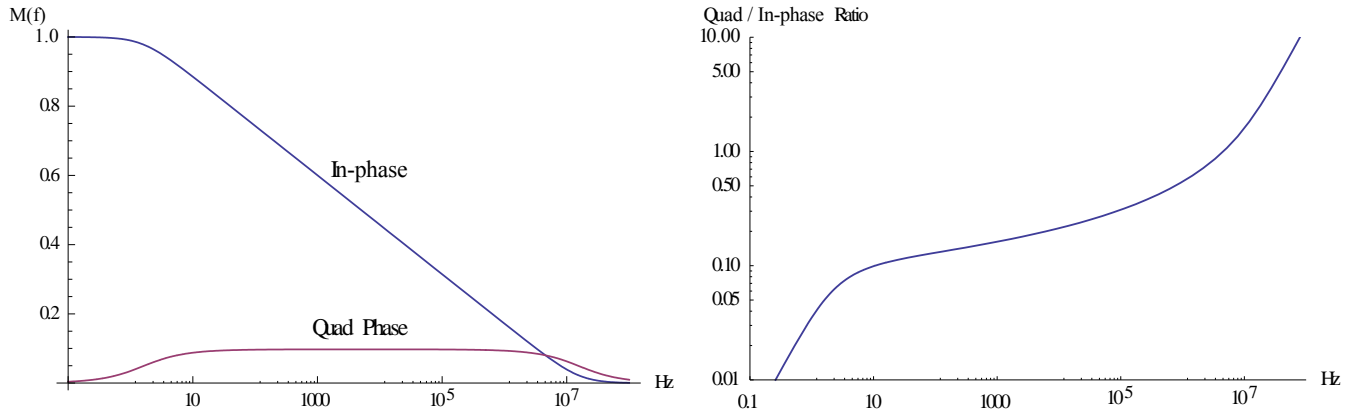## 5. 'Finite Continuous Distribution of Time-Constants' Susceptibility Model

To date we have discussed two models, (1) the 'finite discrete time-constant' model and (2) Néel's 'infinite continuous distribution of time-constants' model for describing the frequency dependence of the magnetic susceptibility of soils. The author has recently learned that Lee (1983) describes another analytical model for a 'finite continuous distribution of time-constants'. The frequency dependence for this model, in which there is a continuous distribution of time-constants, but only within the range $\tau_1 \rightarrow \tau_2$ (where $\tau_2 > \tau_1$) is given by the expression

$$M(\omega) = M_0 \left[1 - \frac{1}{\ln(\tau_2/\tau_1)} \ln\left(\frac{1 + i\omega\tau_2}{1 + i\omega\tau_1} \right) \right]. \tag{11}$$

From equation (12) Pasion et al (2003) have derived that the slope of the in-phase component of this function is given by another useful expression

$$Slope = \frac{\partial M(\omega)}{\partial \ln(\omega)} = -\frac{M_0}{\ln(\tau_2/\tau_1)} . \tag{12}$$

Most papers describing the 'finite continuous distribution of time-constants' model assume that the range of time-constants extends from about $\tau_1 = 10^{-8} \sec$ to $\tau_2 = 0.1 \sec$. Plots of $M(f)$ and the quadrature/in-phase ratio (calculated from equation (11) for these values of τ) are given below. These plots are to be compared with the plots for the 'finite discrete time-constant' responses on pages 6 and 7 (noting that on those pages the time-constants were $\tau_1 = 10^{-6} \sec$ and $\tau_2 = 1 \sec$).

9

Apart from the anticipated smoothness of the new model, all features of the earlier 'finite discrete time-constant' model are preserved. Moreover when the range of time-constants is very large this model also accurately reproduces all features of the Néel model, including the defining relationship of equation (10) as long as the calculation is done in the vicinity of the geometric centre of the frequency distribution, defined as

$$ f_{gc} = 1/(2\pi \sqrt{(\tau_1 \tau_2)}). \tag{13} $$

Indeed, as seen from the plot, for a large range of $\tau_1 \to \tau_2$, both the quadrature phase component and the slope of the in-phase components are essentially constant with frequency so that equation (10) also applies over a wide frequency range.

The applicability of this model to measured data will be demonstrated in the next Section.
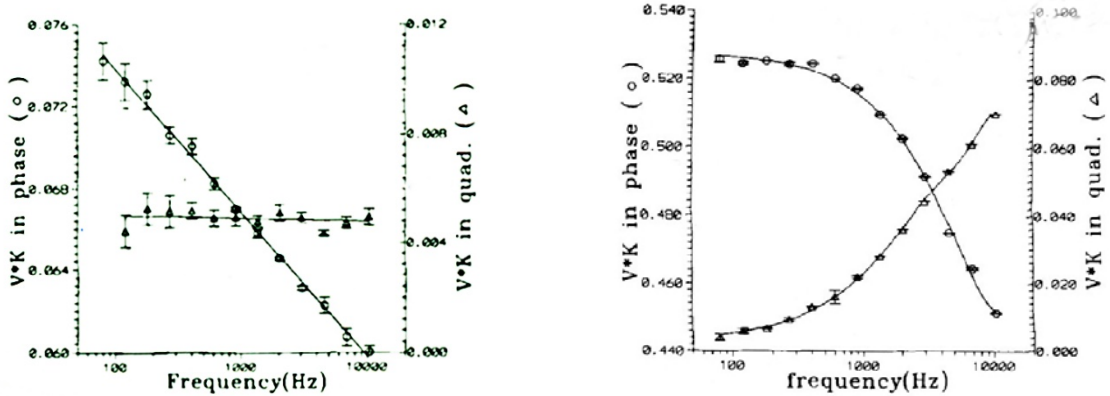
6. Comparison of Laboratory Measurements of Magnetic Susceptibility with Theory

Dabas et al (1992) have made accurate measurements of the in-phase and quadrature phase susceptibility of more than 50 soil samples from a wide variety of archaeological sites, all of which showed anomalous electromagnetic response, over a wide range of frequencies from $80\,Hz$ to $10.3\,kHz$.

Susceptibility of the majority of their samples (an example of which is shown on the left side of the figure below) showed agreement with all aspects of Néel theory for an infinite assemblage of time-constants, including that equation (10) was fully satisfied.
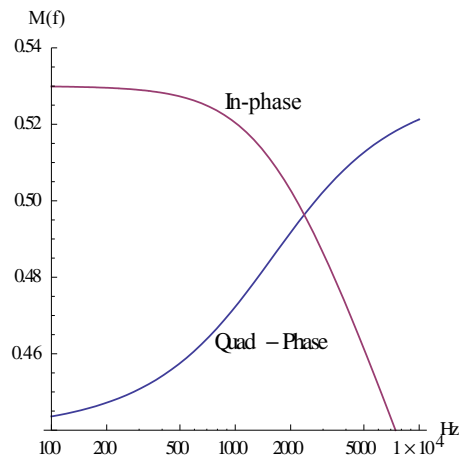
A smaller number of samples, however, exhibited 'anomalous' behavior as shown on the right side of the figure. These authors were unable to explain this type of response.

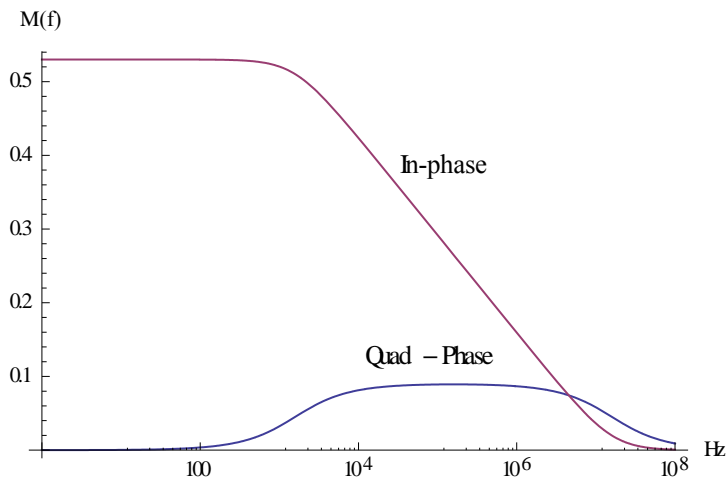On each figure note that the left scale refers to the in-phase component (trace decreasing with

frequency) and the right scale to the quadrature phase component (trace constant or increasing with frequency) with different scale values for each plot. V*K is cgs sample-volume times susceptibility.

For comparison with the 'anomalous' data the figure below shows calculated results for $M(f)$
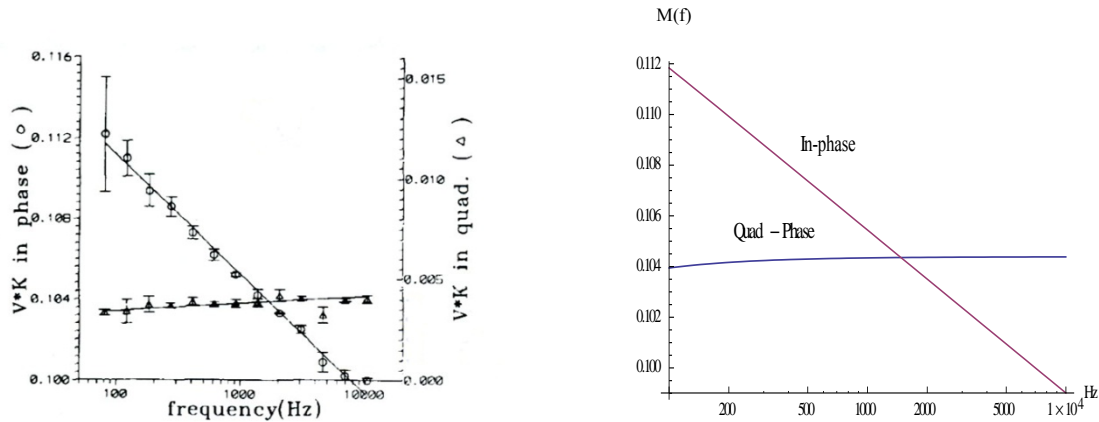

using equation (11) that are seen to give an excellent fit to the measured data. The range of time-constants extended from $\tau_1 = 10^{-8}$ sec to $\tau_2 = 10^{-4}$ sec ; static susceptibility M_0 was 0.53 units. Scales have been shifted and the frequency range chosen so as to allow direct comparison with the Dabas et al data.

The next figure shows the same calculated curves, but now over a wider frequency range and

11

with scales again adjusted to facilitate comparison with the earlier figures in Section 3 and Section 5.

Dabas et al also encountered a few samples which exhibited another unexplained 'anomalous' response, differing in that the quadrature phase susceptibility increased slightly with frequency, as shown on the left side of the next figure.
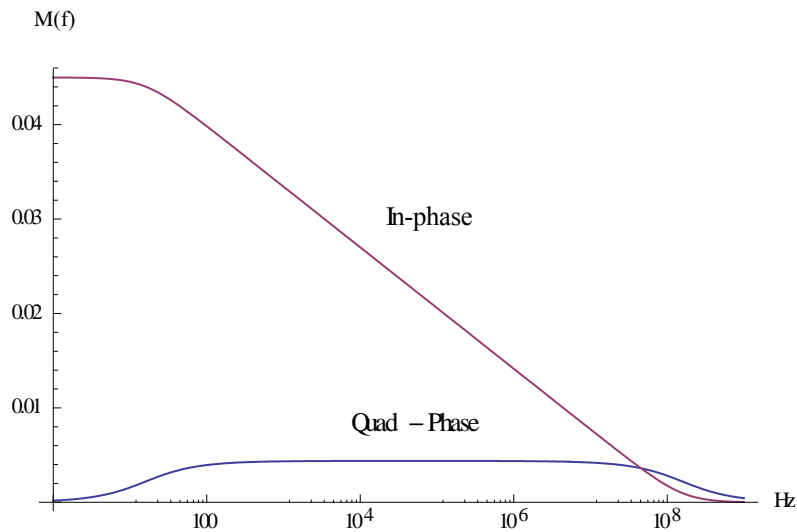

Shown in the right-hand side is the calculated response from equation (11), this time for a model in which τ ranged from $\tau_1 = 10^{-9} \sec$ to $\tau_2 = 10^{-2} \sec$. Once again the calculated data have been shifted so as to allow direct comparison with the Dabas et al data.

In this case good agreement with the measured data could only be achieved if a frequency-invariant component of magnetic susceptibility of amplitude 0.072 units was subtracted from the calculated in-phase data. As we have seen from our earlier 'finite discrete time-constant' model there is no reason why such a constant, in-phase-only (no viscous magnetism) susceptibility component should not exist along with a viscous magnetic susceptibility component. Different grain sizes are known to give different types of response, some of which show no quadrature component (see Section 11) and if well dispersed physically their responses will all add linearly to the viscous component.

The agreement between the measured and calculated models is again excellent.

The figure below again shows the calculated curves for the same data to facilitate comparison with the earlier models of Sections (3) and (5).
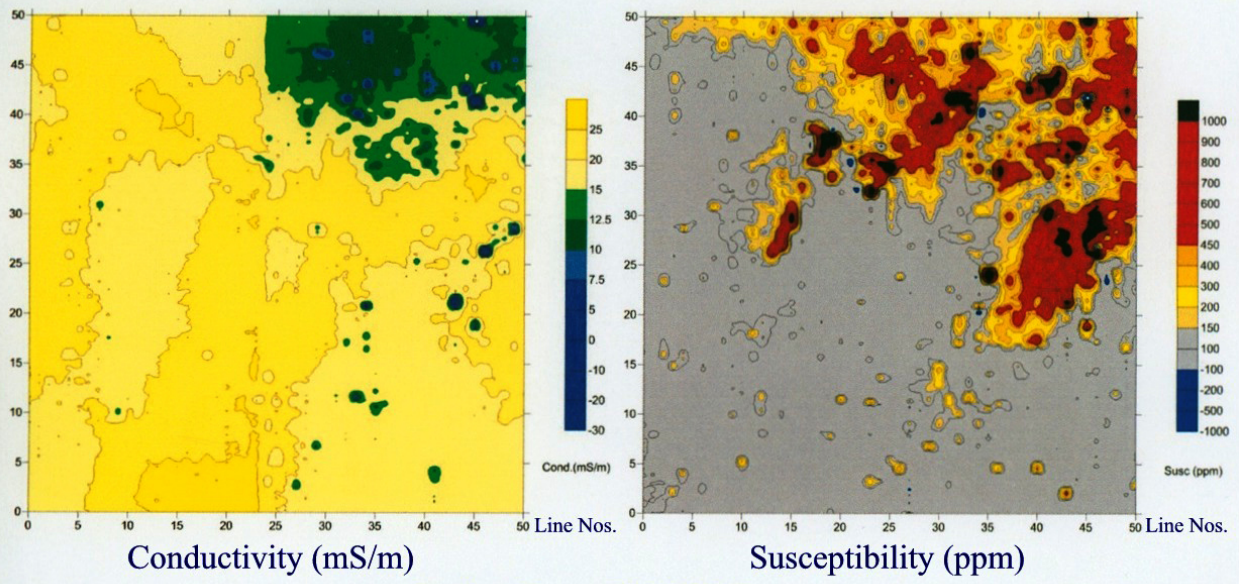
At the start of this Section it was mentioned that Dabas et al stated that the susceptibility of the majority of their samples (i.e. all of those that were not 'anomalous') showed agreement with all aspects of Néel theory for an infinite assemblage of time-constants. This means that all of these samples would also be described by the finite continuous distribution of time-constants described in Section (5) since that model easily incorporates the responses predicted by Néel theory. Moreover we have shown that this model also easily incorporates the anomalous responses obtained by Dabas et al, which are not described by Néel theory. Finally, most measurements of soil susceptibility reported by other workers (which were generally done over a narrower frequency range) also obeyed the Néel theory and so would be described by the theory of Section (5).
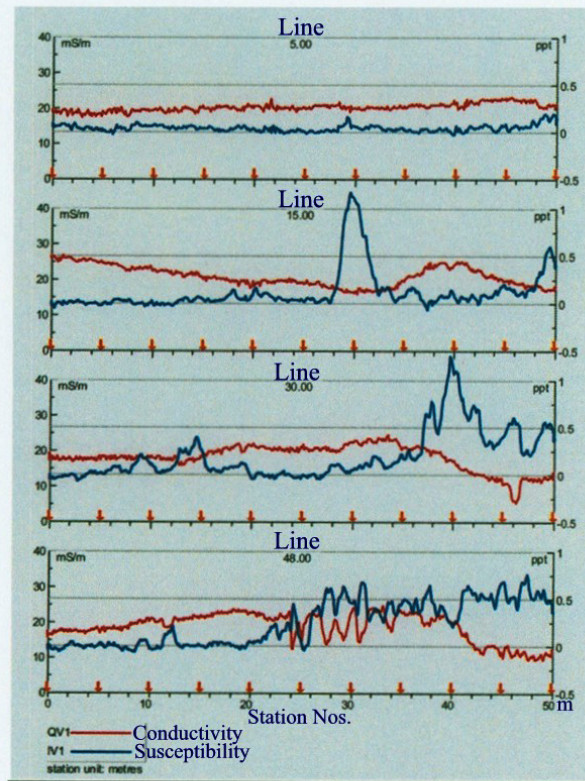
7. Magnetic Susceptibility Survey Data from the EM38B

It was stated above that the Néel theory was in good agreement with measured data on various soil samples taken from different archaeological sites by many workers. Our problem is that in many instances it does not explain some of the susceptibility/conductivity survey data taken with the EM 38B, such as that from the Thibodeau Village site on the Ste-Croix River in Nova Scotia.

Initial settlement at the Thibodeau Village may be inferred from census records to have been established between 1690-93 by Pierre Thibodeau and Anne-Marie Bourg (Fowler, 2000; White, 1999). While the settlement is depicted on several mid-18th century British maps, it was never the focus of mapmakers' attention, and consequently was only rendered at small scales, appearing as a single symbol or as a cluster of dots.

13

Conductivity (mS/m)   Susceptibility (ppm)

Poplar Grove EM 38B Survey

Little is known about the fate of the village, whose inhabitants were deported to Massachusetts by Anglo-American forces in 1755 as part of the overall deportation of all Acadians from the Province. The site's present occupants descend from the New England Planters, who settled in Nova Scotia in the 1760s at the behest of a British colonial government eager to fill the demographic void left by the removal of the Acadians, who had lived in the Province for the previous hundred years (Beanlands, 2010). Above ground, little if any evidence of the Thibodeau village remains.

The Thibodeau Village survey area, shown in plan view on the preceding page, is 50 X 50 m in size. Terrain magnetic susceptibility and electrical conductivity were measured simultaneously along 51 N/S survey lines (vertically directed on the page) each spaced 1 m apart. Data were taken automatically at about 25 cm intervals along each survey line.

It should be noted that there was virtually no information about the survey area before the actual survey. The very active susceptibility plot was quite a surprise since most survey areas produce only a few susceptibility anomalies in this relatively unpopulated but historical region of Nova Scotia!

The two data plots appear to be almost completely unrelated. This observer is always amazed that measurement of two components (in-phase and quadrature phase) of a simple sinusoidal response can yield such totally different sets of data.

The conductivity data is generally slowly varying over the survey area and the values of conductivity, varying about three or four mS/m from the average value of about 20 mS/m, are quite typical for surveys in this part of Nova Scotia. Data correlation from line-to-line is normally very good as shown here.

An exception occurs in the north-eastern part of the survey area, where the conductivity drops quite abruptly by about 5 mS/m throughout a broad, rectangular area 25 m in the E/W direction and somewhat less than 10 m in the N/S direction.

There are also several very small anomalies dispersed throughout the area, visible as small green circles on the plan map.

The susceptibility data is entirely different. For nearly three-quarters of the survey area the values are very low, in the range of about 100 ppm, and line-to-line correlation is good. On the other hand responses in the north-eastern part of the survey area are of very high value, many 100's and even over 1000 ppm, and are extremely patchy, changing abruptly over small distances in the survey area. Line-to-line correlation is often poor to non-existent.

Particular features of this data are illustrated more clearly in the survey profiles for lines 5, 15, 30, and 48 in the bottom half of the previous page. Note that the scale for quadrature phase/conductivity (red profile) is on the left half and in-phase/susceptibility (blue profile) is on the right half of the figure. Unlike the plan view, the profile scale for susceptibility is in ppt rather than ppm; 0.5 ppt=500 ppm etc. The profile conductivity 'zero' level is at the bottom of the graph whereas the susceptibility zero has been offset upwards by 0.5 ppt to facilitate comparison of the two types of response. Moreover the scale for

the conductivity data range (0 to 40 mS/m) has been chosen so that both scales are roughly equivalent in ppt since 30 mS/m is about 1 ppt of quadrature phase response.

The profile for line 5 is typical for many survey areas in that susceptibility anomalies are normally few and far between. The profile noise levels are about 0.05 ppt for susceptibility and 1 mS/m (equivalent to 0.03 ppt) for conductivity, which are slightly higher than normal. This profile gives a good idea of the background values against which anomalous areas are to be detected. Anomalous susceptibility values are normally of the order of 0.2/0.3 ppt and often only slightly higher.

We see, then, that lines 15, 30 and 48 are very anomalous, with several different types of anomaly response.

Line 15, for example, shows a large, more-or-less continuous in-phase anomaly at station 30 and several smaller in-phase anomalies, none with indication of any accompanying quadrature phase anomalies.

The same applies to line 30, except that the susceptibility anomaly at station 46 shows a small negative conductivity (quadrature phase) anomaly. There is a broad decrease in the conductivity channel which may be associated with the large susceptibility anomaly.

Line 48 shows a small susceptibility anomaly at station 12 with an accompanying negative conductivity anomaly, but more interestingly, a series of susceptibility anomalies from stations 24 to 34, all with associated negative conductivity anomalies. The first of these, which is very sharply defined, is probably a response to metal, but the remaining ones are not. We note that the ratio of quadrature phase to in-phase ratio is about one.

The broad, highly-variable in-phase anomaly, which started at station 20, continues to the end of the line at station 50. If we ignore the rapidly varying, negative-going conductivity anomalies referred to above, we see that once again the conductivity channel decreases abruptly beyond station 40.

Not shown on the selected profiles in the figure above, but quite common in surveys, are anomalies in which the negative going conductivity anomalies associated with susceptibilities are large enough to be clearly seen on the survey plots, examples of which are easily seen on the conductivity plan map as the small circular green anomalies. Although not a problem in the current survey in areas in which susceptibility anomalies abound and in which the terrain conductivity is very low such negative conductivity anomalies can totally dominate the conductivity map, rendering it of little use (Linford, 1998).

Many more examples of survey response are shown in Technical NotesTN34 and TN35.

8. Comments on Survey Data

From the survey data above, we see that there are susceptibility anomalies, both broadly and sharply defined, which are not associated with negative quadrature phase anomalies. These anomalies form the basis of simple susceptibility theory (without relaxation effects).

We also see that there are susceptibility anomalies, both broadly and sharply defined, that are associated with similarly-shaped, negative quadrature phase responses. We see that the quadrature/ in-phase ratio can vary widely from near zero to (less often) one or two. Such anomalies are not permitted from simple susceptibility theory, nor are they permitted by Néel complex susceptibility theory.

With reference to the plot of quadrature/in-phase ratio on page 7, had we assumed, as did Néel, an infinite assemblage there would be no 'wings' on this plot at the extreme lower and upper frequency ranges.   Because of the small slope of this curve, at any frequency within the central portion of the curve there would be little variation in the measured quadrature/in-phase ratio caused by different time-constants. But the measured quadrature/in-phase ratio from our survey data, done at a fixed frequency, consistently shows many anomalous values. There is a problem!
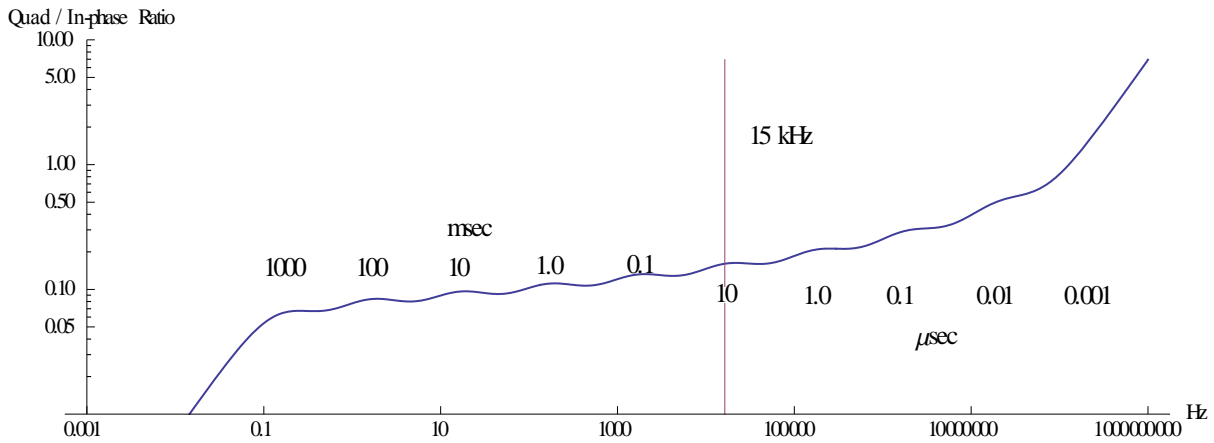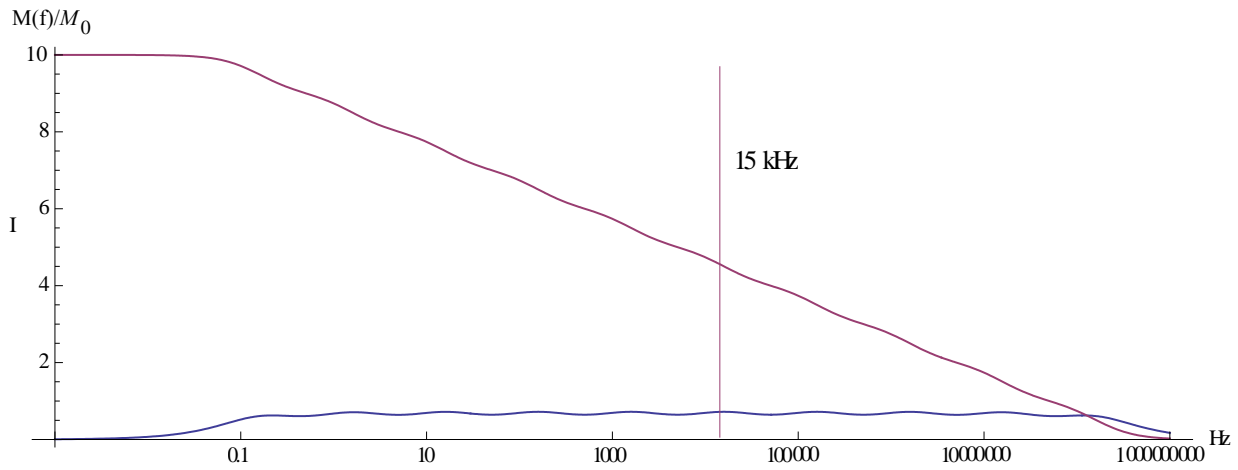
At the operating frequency of $15\,kHz$ it is possible that we might be working at the high frequency end of the curve of page 7, but there is still a problem. That plot shows that in that case we will only see high values of quadrature/in-phase ratio and not the low values of the quadrature/in-phase ratio that we see in practice.

9. Study of Susceptibility Models to Explain the Complex Susceptibility Responses

We have studied the response from many theoretical susceptibility models and have concluded that there are four phenomena that might cause the anomalous quadrature/in-phase responses of the type measured by the EM38B at operating frequency of 15 kHz.
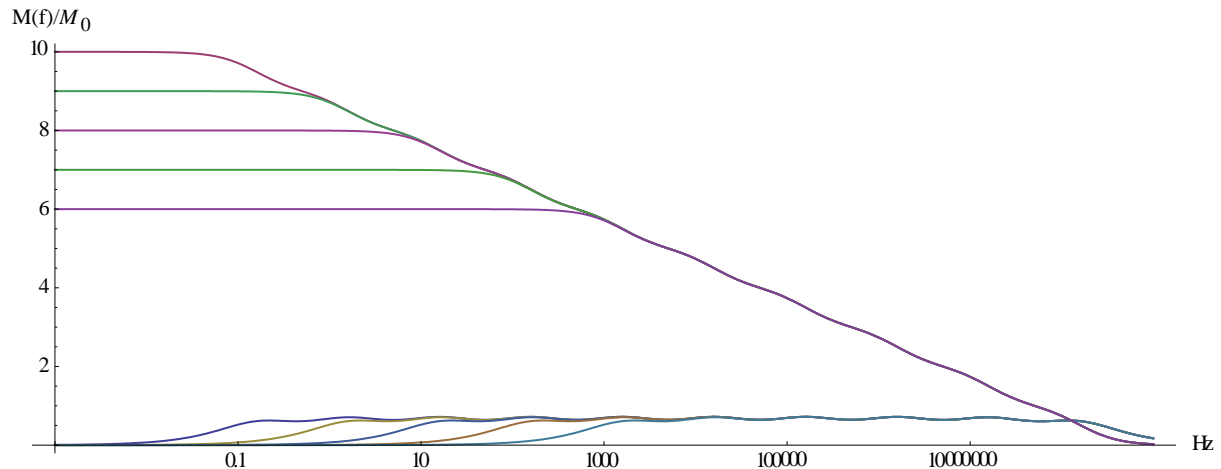
In every case we started with the assumption that there is a background complex susceptibility spectrum of uniform time-constants extending from $10^{-9}\sec$ to $10^{0}\sec$. Such a model produces features that are in agreement with Néel theory and we know that many laboratory measurements (both in the frequency-domain and in the time-domain) of magnetic susceptibility are in accord with this model (although perhaps only because they were performed over a relatively narrow frequency or time interval). We then examined any deviations from this model that might cause anomalous response exhibiting the variety of quadrature/in-phase ratios that we see in actual frequency-domain surveys.
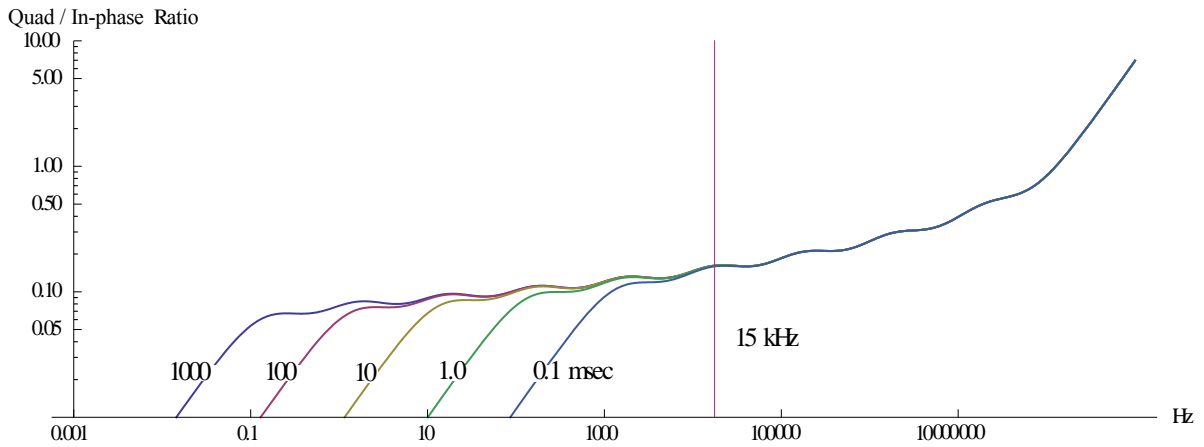
For this study we used the 'finite discrete time-constant' susceptibility model shown below since it is easily modified. Note that in this figure the low-frequency susceptibility is 10 units since we have added ten time-constants, each of low-frequency amplitude one unit.

Both figures show location of the EM 38B operating frequency (since it is at this frequency that we are searching for changes in the quadrature/in-phase ratio). The quadrature/in-phase ratio figure also shows the location of each of the ten time-constants.
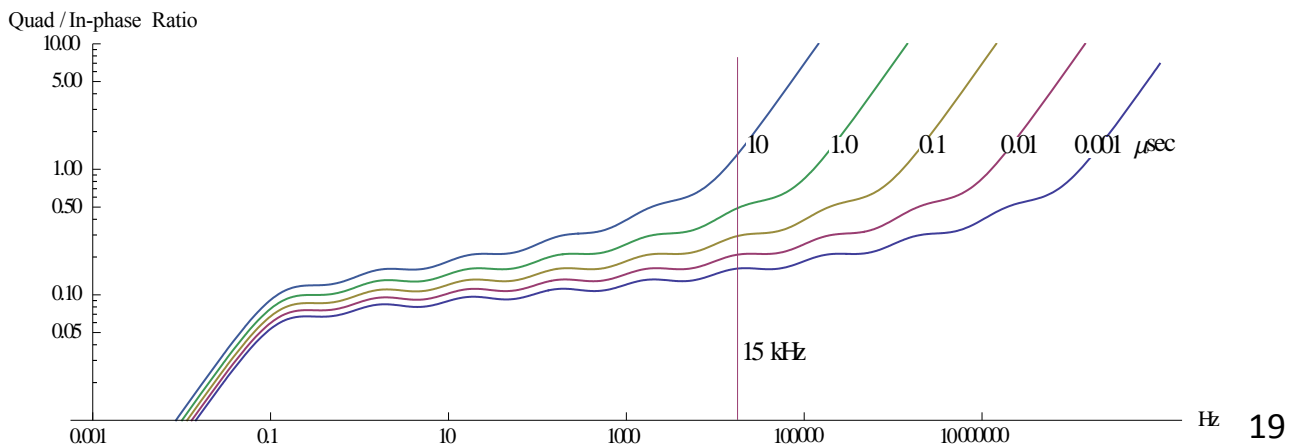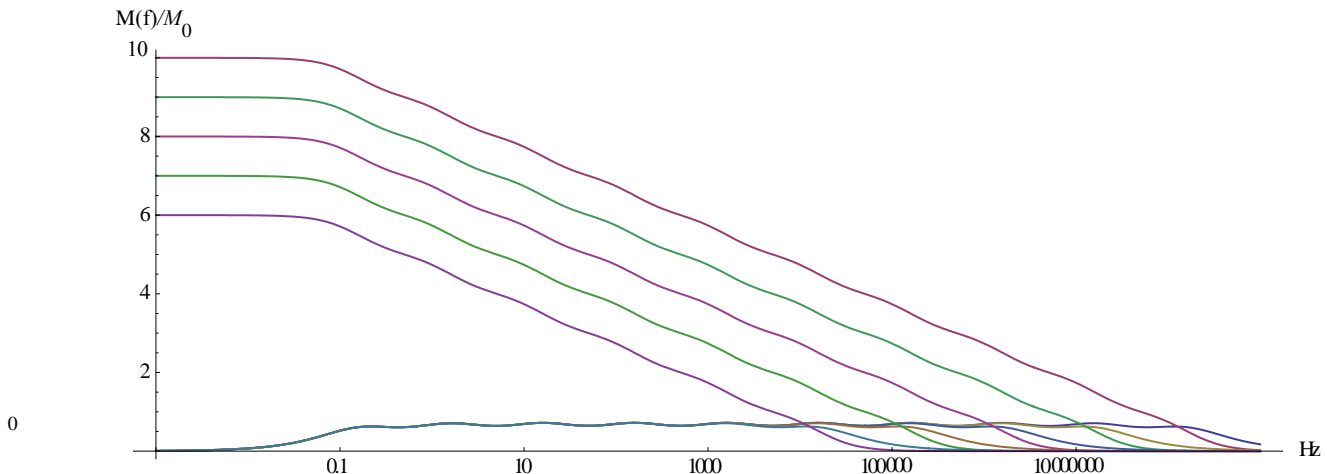
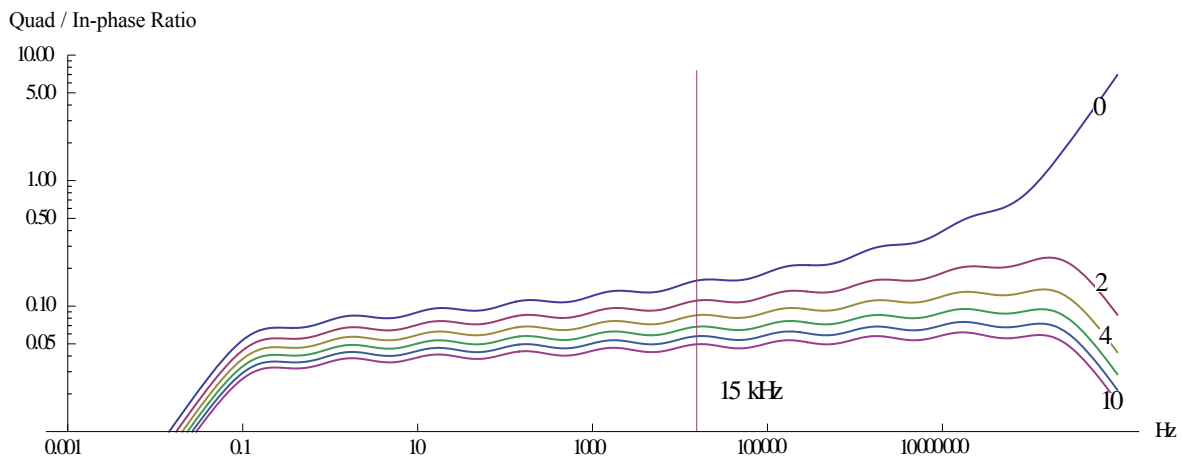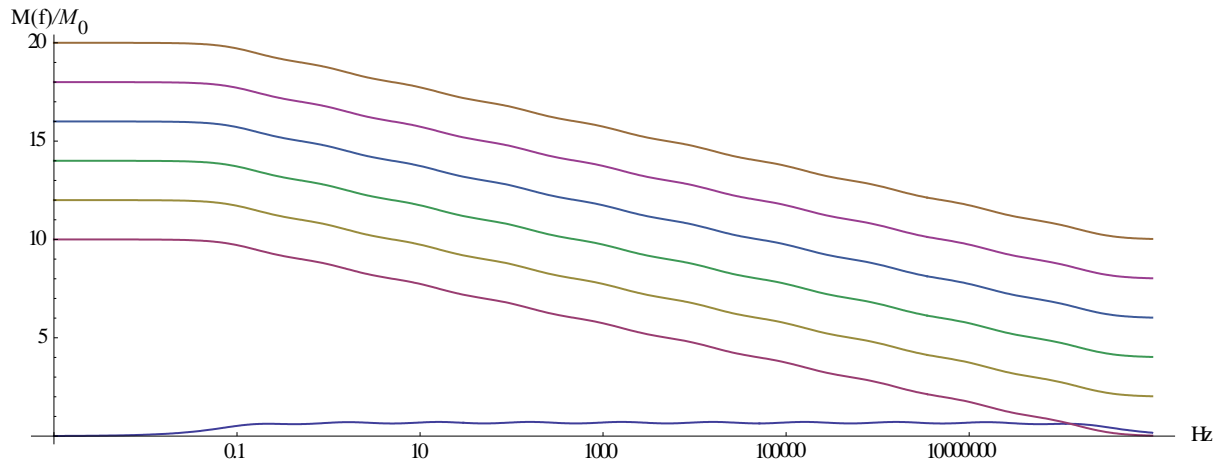9 (1) Removal of the Largest Time-Constants

18

For this modification we have successively removed the four largest time-constants shown on the figure above. We see that there is virtually no effect on the quadrature/in-phase ratio at 15 kHz. The reason is obvious from the single time-constant figure on page 4, where we see that both the quadrature and the in-phase responses fall off rapidly with higher frequencies once we are well above the peak frequency. We conclude that variations in the longest time-constants do not produce the quadrature/in-phase variations seen in EM 38B survey data.

9 (2) Removal of the Smallest Time-Constants

For this modification we have successively removed the five smallest time-constants shown on the figure above, which we see has a large effect on the quadrature/in-phase ratio. From the single time-constant figure on page 4 we see that the in-phase response is large below the peak frequency and changes made by removing higher frequencies will have a pronounced effect on the in-phase response at lower frequencies and thus the quadrature/in-phase ratio at lower frequencies.   We conclude that variations in the number of shortest time-constants will produce quadrature/in-phase variations of the type seen in EM 38B survey data.
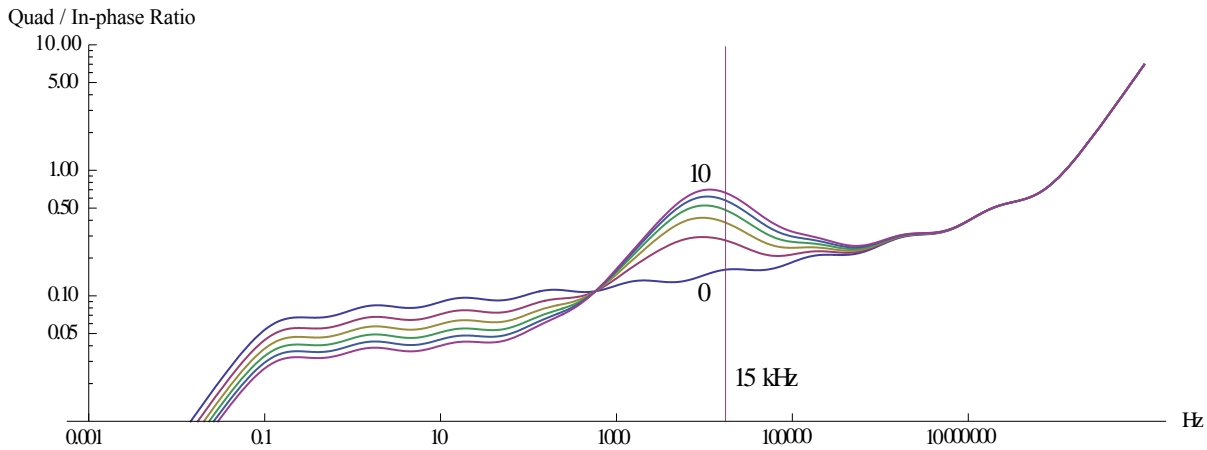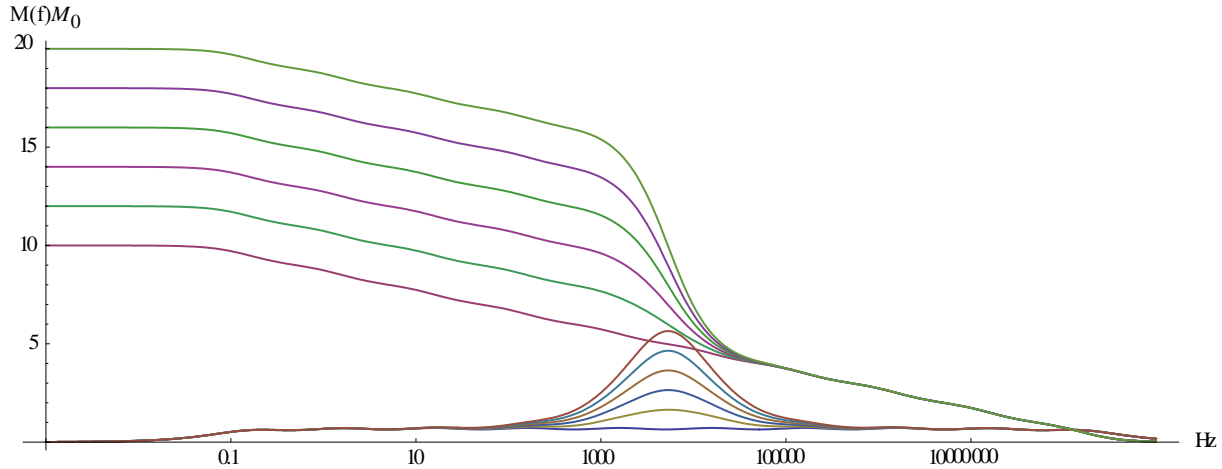
9 (3) Addition of a Frequency-Independent In-phase Component

For this modification we have successively added a frequency-independent, in-phase component of amplitude 2 times, 4 times, and up to 10 times the amplitude of the quadrature phase component amplitudes, equivalent to 20%, 40% etc. of the in-phase component of ten units. It is quite possible that in practice an in-phase component of even higher amplitude may exist, however we note that at 15 kHz the quadrature/in-phase ratio is already low, and is further reduced by the frequency-independent, in-

phase component. We conclude that variations in the amplitude of a frequency-independent, in-phase component do not produce the quadrature/in-phase variations seen in EM 38B survey data.

9 (4) Addition of a 30 Microsecond Time-Constant Anomaly of Varying Amplitude
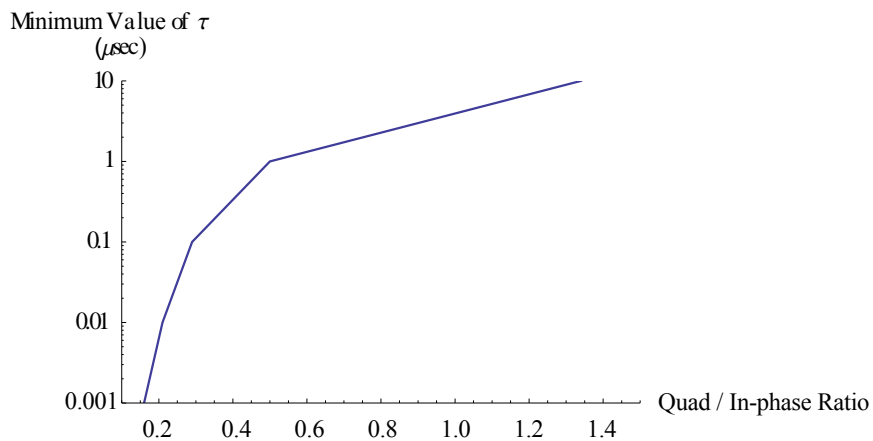
$M(f) M_0$

Quad / In-phase Ratio

For this modification we have successively added a $30 \mu \sec$ (τ chosen to give a very high response at 15 kHz) single time-constant of amplitude 0 times, 2 times, 4 times, and up to 10 times the amplitude of the quadrature phase component amplitudes. We conclude that such an anomaly will produce the quadrature/in-phase variations seen in EM 38B survey data. Of course other large anomalies of time-constants in the vicinity of $30 \mu \sec$ will also produce variations in the quadrature/in-phase ratio if they have significant response at 15 kHz.

Using our model of ten discrete time-constants we have examined four possible sources of the type of quadrature phase response found in EM 38B susceptibility surveys. Of these (1) wholesale removal of the short time-constant components (time-constants in the low microsecond to sub-microsecond range) of the distribution and/or (2) the existence of any discrete time-constant anomalies with a significant response at 15 kHz will generate quadrature phase responses. While there is certainly no guarantee that, as assumed by Néel, the overall time-constant distribution will be of uniform amplitude, many measurements have suggested that this is often the case, especially when measured over relatively narrow frequency ranges. Moreover the 'finite time-constant' model examined in Section 3 reveals that the response of any one time-constant influences such a broad frequency range that the overall variation in the spectral distribution may be rather small. And finally, as shown by equation (1) and further demonstrated below, the extreme sensitivity of relaxation time-constant to grain size will certainly mitigate against narrow, localized time-constant anomalies since, as we will see, a very narrow distribution of different grain sizes produces an enormously wide range of different time-constants. Localized time-constant anomalies would require an incredibly narrow spectrum of grain sizes.
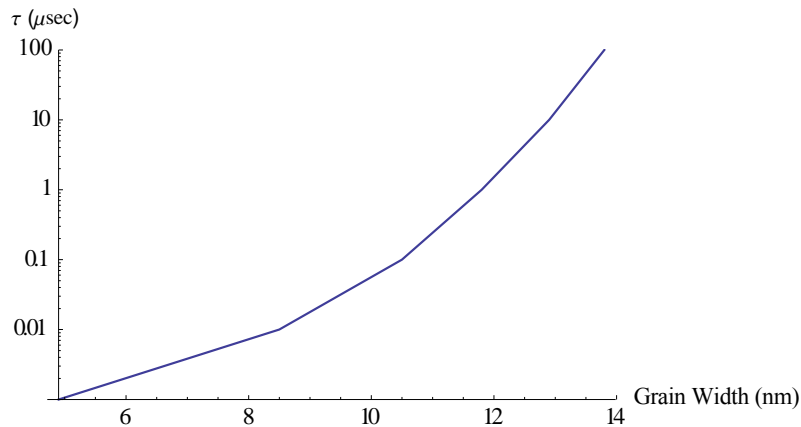
For these reasons we prefer the argument that it is wholesale removal of short time-constant components that is probably causing the quadrature-in-phase anomalies seen by the EM 38B, rather than the presence of localized anomalies.

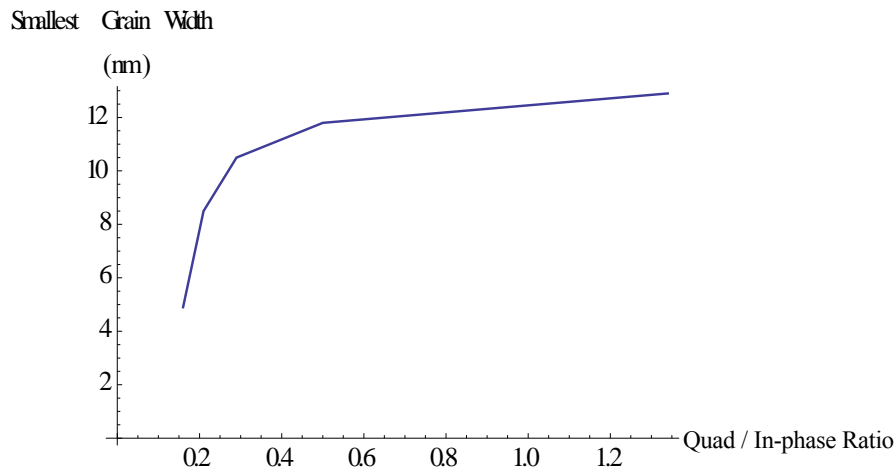### 10. A Possible Method to Measure Minimum Grain Volume in a Distribution of Grain Volumes

We examine the model shown in Section 9(2) in more detail. The quadrature-in-phase data shown in that Section can be replotted as shown below to give the value of the smallest time-constant (in the distribution of time-constants) as a function of quadrature/in-phase ratio measured at frequency of $15\ kHz$.

Tauxe (2010), using equation (1) from Néel with parameters appropriate for magnetite at normal ambient temperature, presents an interesting graph showing how the relaxation time-constant (τ) depends on grain width for magnetite grains with fixed length/width ratio of 1.3/1. We recalculate and replot Tauxe's data below at expanded scale to show greater resolution for very short time-constants. As demonstrated by equation (1) a small spread in grain width produces an enormous spread in relaxation time-constant. Since it seems very unlikely that an essentially mono-disperse distribution of grain sizes would occur in nature, this graph confirms that 'localized' time-constant anomalies would be equally unlikely.

Finally, combining the two plots above we now construct an important plot of the smallest magnetite grain-width (in the grain size distribution) as a function of quadrature/in-phase ratio, as shown below.

At least in theory this graph shows that the smallest grain width that is present in the overall spectrum of grain widths is determined by the measured quadrature/in-phase ratio measured at $15\,kHz$.

With no claim to expertise in mineral magnetic susceptibility, we cautiously suggest that measurement of the quadrature/in-phase ratio with an EM 38B may allow determination of the smallest grain width in the size distribution. We look forward to comments on this suggestion.

11. A Note on Possible Mechanisms for Quadrature-Free Susceptibility Response

It was stated in Section 7 that many responses showed no quadrature phase component at all. It appears that the reasons for this also stem from particle grain size/volume. It is thought that the 'viscosity effects' described above occur in the range of grain diameters between approximately 10 and 100 nm, for within this range, and at ambient temperature, equation (1) predicts time-constants, the reciprocal of which are comparable to the frequencies at which many measurements of soil susceptibility are made, and which will thus cause viscous effects in these measurements.

On the other hand equation (1) predicts that the smallest grain sizes will be such that the numerator in the exponent in this equation will be less than kT, which means that the thermal energy of the grains will significantly exceed the barrier energy, and the domains will easily rotate in the presence of an external magnetic field with no delay. Since J_s, the spontaneous magnetic moment of a single-domain grain is very large, rotation of a single-domain grain produces a large increase in the induced magnetic field and thus of the magnetic susceptibility. This behavior, known as 'superparamagnetism' will not produce a quadrature phase response.

Another source of quadrature-free susceptibility may arise from much larger grain sizes, typically of the order of μm size. These grains are large enough for 'multi-domain' behavior in which the interior regions of the grain are divided into many domains so as to reduce the internal energy; each domain is separated by a domain wall. When an external magnetic field is applied to the grain, the inter-domain walls translate allowing the domains within the grain to rotate. Such translation takes much less energy than rotating a single domain across the energy barrier described in Section 2. Although the subsequent increase in grain susceptibility will not be as large as for single domain or superparamagnetic behavior (not all grains need to rotate in the multi-domain configuration) the response will be nearly instantaneous and once again there will be much less or no quadrature phase component to the response.

Clark (1989) suggests that multi-domain behavior is often a characteristic of material directly weathered from bedrock, whereas the "processes of reworking by man (including burning) tends to favour change to the smaller grain sizes" which are the source of magnetic viscosity.

12. Summary and Conclusions

In this Technical Note we have examined various theoretical models of the magnetic susceptibility of soils to see whether they could explain survey data taken with the Geonics EM 38B over many years at various archaeological sites in Nova Scotia. We have described the data from one such site to

illustrate the unexplained localized quadrature phase anomalies which are quite common in all of our survey data.

We have shown that none of the current theoretical models can explain this feature, nor do most of the published laboratory measurements of soil susceptibility show this feature. In general a great majority of the measurement data can be satisfactorily explained by the current models. However a few of the measurements may suggest a similar response.

It is suspected that the reason for the lack of agreement between theory, other measurements and our survey data is that (1) our data are taken at a higher frequency than the laboratory measurements, and (2) the theory simply does not encompass the phenomenon that we are seeing.

We have studied a series of modifications to the theoretical models that might expand them to incorporate our survey data. Two of the four modifications would not explain our data, a third would, but seemed very unlikely in view of what is known from the models about the complex nature of soil susceptibility.

The fourth modification does seem to explain our survey data, and moreover we describe a method for calculating the smallest possible magnetite grain width existing in the otherwise more or less continuous sequence of grain widths predicted by current theoretical models.

We conclude that survey evidence arising from the EM 38B indicates that reported laboratory measurements of soil susceptibility have probably been carried out over too limited a frequency range to fully explore the behavior of susceptibility in typical soils.

Our particular interest in all of this stems from the accepted fact that the magnetic susceptibility of archaeological sites is enhanced by human activity, particularly burning. We think that it is important to learn more about the influence of burning on the grain size spectrum of ferromagnetic minerals such as magnetite. It may be that, as suggested by Clark and described in Section 11, this can be accomplished by making laboratory measurements of magnetic susceptibility on soils from areas known to have been burnt.

Of course we would also like to confirm that field measurements of the quadrature/in-phase ratio of magnetic susceptibility at archaeological sites are related to minimum grain size as has been suggested in this Technical Note. Should this be correct there may be an excellent opportunity to identify burnt areas from surface measurement of the complex magnetic susceptibility

Acknowledgements

Sylvia who has assisted me in carrying out many surveys, who has been unbelievably patient as I poured over survey data and wrote Technical Notes, and who is still trying to figure out what "retirement" really means.

Bibliography

Beanlands, S., (2010). "Neighbours in Time", in "Underground Nova Scotia: Stories of Archaeology", (Erickson, P.E., and Fowler, J., eds.) Halifax, Nimbus Publishing, 35-42.

Clark, A., (2000). "Seeing Beneath the Soil". Routledge, Abingdon, Oxen, OX14 4RN; 100-104. Dabas, M., Jolivet, A., Tabbagh, A., (1992). Magnetic Susceptibility and Viscosity of Soils in a Weak Time-Varying Field.   Geophys. J. Int., (1992) 108,101-109.

Fowler, J., (2000). The Minas Environs Project: 2nd Annual Report, 1999-2000. Manuscript Report on File at the Heritage Division, Nova Scotia Department of Communities, Culture and Heritage.

Lee, T., (1984). The Effect of a Superparamagnetic Layer on the Transient Electromagnetic Response of a Ground. Geophysical Prospecting, 32, 480-496.

Linford, N.T., (1998). Geophysical Survey at Boden Vean, Cornwall, Including an Assessment of the Microgravity Technique for the Location of Suspected Archaeological Void Features. Archaeometry. 40, 1, 187-216.

Mullins, C.E., and Tite, M.S., (1973). Magnetic Viscosity, Quadrature Susceptibility, and Frequency Dependence of Susceptibility in Single-Domain Assemblies of Magnetite and Maghemite. J.Geophysical Res. 78, 5; 804-809.

Néel, L., (1949). Theory of the Magnetic After-Effect in Ferromagnetics in the Form of Small Particles, with Applications to Baked Clays. Paper is available in translation in " Selected Works, Louis Néel," Ed. Nicholas Kurti, Routledge, 1988.

Pasion, L.R., Billings, S.D., Oldenburg, D.W., (2003). Evaluating the Effects of Magnetic Susceptibility in UXO Discrimination Problems. Proceedings of the UXO/Countermine Forum, (Orlando, Florida), Sept. 2002. (Also available on the internet).

Tabbagh, A., (1986). Applications and Advantages of the Slingram Electromagnetic Method for
    Archaeological Prospecting. Geophysics. 51, 3; 576-584.

Tauxe, L., (2010). "Essentials of Paleomagnetism". U. of California Press, Berkeley, CA., 60-62.

White, S.A., (1999). Dictionnaire Généalogique des Familles Acadiennes, Moncton: Université de
    Moncton; 1511-13.